Biochemical and Biophysical Research Communications 420 (2012) 492–497

Contents lists available at SciVerse ScienceDirect

Biochemical and Biophysical Research Communications

journal homepage: www.elsevier.com/locate/ybbrc

KCC2 transport activity requires the highly conserved L_{675} in the C-terminal β1 strand

Annika Döding [1], Anna-Maria Hartmann, Timo Beyer, Hans Gerd Nothwang *

Abteilung Neurogenetik, Institut für Biologie und Umweltwissenschaften, Carl von Ossietzky Universität Oldenburg, Oldenburg, Deutschland

ARTICLE INFO

Article history:
Received 17 February 2012
Available online 3 March 2012

Keywords:
Chloride homeostasis
Inhibitory synapse
Regulation
HEK-293
Cation-chloride cotransporter
Evolution

ABSTRACT

The activity of the neuron-specific K^+, Cl^- co-transporter 2 (KCC2) is required for hyperpolarizing action of GABA and glycine. KCC2-mediated transport therefore plays a pivotal role in neuronal inhibition. Few analyses have addressed the amino acid requirements for transport-competent conformation. KCC2 consists of 12 transmembrane domains flanked by two intracellular termini. Structural analyses of a related archaeal protein have identified an evolutionary extremely conserved β1 strand, which links the transmembrane domain to a C-terminal dimerization interface. Here, we focused on the sequence requirement of this linker. We mutated four highly conserved amino acids of the β1 strand ($_{673}$QLLV$_{676}$) to alanine and analyzed the functional consequences in mammalian cells. Flux measurements demonstrated that L_{675A} significantly reduced KCC2 transport activity by 41%, whereas the other three mutants displayed normal activity. Immunocytochemistry and cell surface labeling revealed normal trafficking of all four mutants. Altogether, our results identify L_{675} as a critical residue for KCC2 transport activity. Furthermore, in view of its evolutionary conservation, the data suggest a remarkable tolerance of the KCC2 transport activity to amino acid substitutions in the β1 strand.

1. Introduction

Cation-chloride-cotransporters (CCCs) are electro neutral secondary-active transporters, which participate in essential physiological processes such as epithelial salt transport, osmotic regulation, and Cl^--homeostasis [1]. CCCs are divided into Na^+, K^+, Cl^- inward transporters (NKCC1-2, NCC), K^+, Cl^- extruders (KCC1-4), a polyamine transporter (CCC9), and the cotransporter-interacting protein CIP1 [1,2]. Among the KCCs, the neuron-specific KCC2 plays an outstanding role, as its activity is required for the hyperpolarizing action of the inhibitory neurotransmitters GABA and glycine [3–8]. In accord with this essential role, $KCC2^{-/-}$ mice die perinatally due to respiratory failure in the absence of synaptic inhibition [5], and knocking-down of the transporter leads to generalized seizure [9,10].

The structural organization of transport-active CCCs is highly conserved. The functional units are oligomers [11,12] and the individual genes encode polypeptides consisting of 12 transmembrane domains (TMD), a large extracellular loop (LEL), and intracellular termini [1]. Evolutionary sequence conservation is highest in the TMDs, followed by the C-terminus, whereas the N-terminus is poorly conserved [1,13]. Functional analyses of NKCCs revealed that TMD 2, 5 and 7 are necessary for the ion binding and transport [14–16]. The termini and the LEL are involved in allosteric or regulatory effects [16–18]. Concerning KCC2, several sites critical for its transport-active conformation have been identified. Mutation of the four cysteines in the LEL [18] or mutation of the C-terminal Y_{1087} to aspartate drastically reduced transport activity [19], whereas mutations that mimicked the dephosphorylated state of T_{906}/T_{1007} increased transport activity [20]. Finally, a KCC2-specific ISO domain was identified, which is involved in constitutive activity under isotonic conditions [21].

Recently, the X-ray structure of the C-terminus of a prokaryotic CCC (*Methanosaccrina acetovirans*, *ma*CCC) was determined [13]. This analysis revealed that the C-terminus is organized into two antiparallel subdomains, each composed of five parallel β-sheets, connected by α-helices. Notably, the highest evolutionary sequence conservation in the entire C-terminus was observed for the β1 strand [13]. To analyze the importance of this evolutionary conservation, we performed mutational analyses in the rat KCC2 (*rn*KCC2). Four highly conserved amino acids ($_{673}$QLLV$_{676}$) of the β1 strand were replaced by alanine and the functional consequences studied in mammalian cells.

* Corresponding author. Address: Abteilung Neurogenetik, Carl von Ossietzky Universität Oldenburg, D-26111 Oldenburg, Deutschland. Fax: +49 441 798 3250.
E-mail address: hans.g.nothwang@uni-oldenburg.de (H.G. Nothwang).
[1] Present address: Institut für Allgemeine Zoologie und Tierphysiologie, Universität Jena, Deutschland.

0006-291X/$ - see front matter © 2012 Elsevier Inc. All rights reserved.
doi:10.1016/j.bbrc.2012.02.147

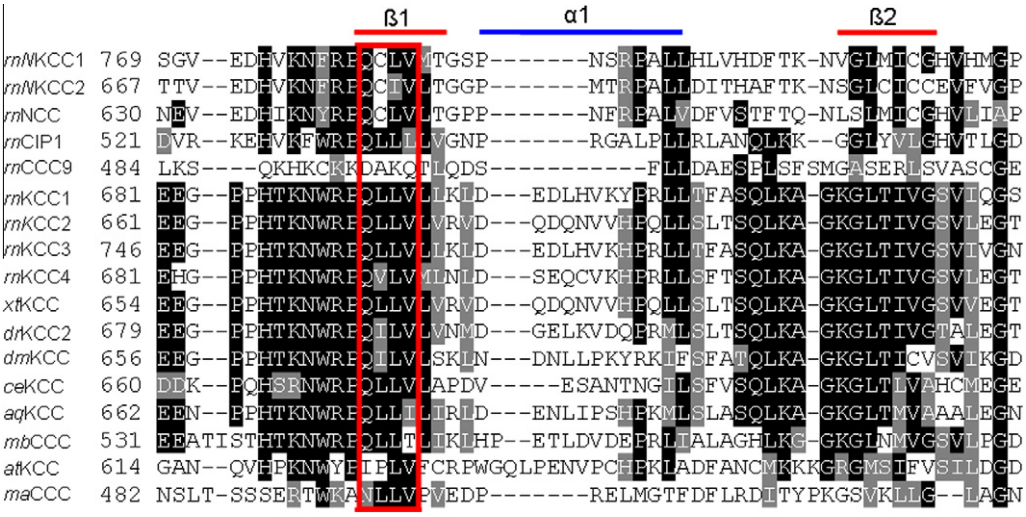

Fig. 1. QLLV residues are highly conserved in the β1 strand structure. A multiple sequence alignment of the C-terminal region of different CCC transporter was made with ClustalW [29]. Secondary structure data were derived from the crystal structure of the C-terminus of a CCC from *M. acetovirans* [13] and are shown above the alignment. QLLV residues are displayed in the box. The beginning of the C-terminus is indicated by an arrow. *Rn*, *rattus norvegicus*; *dm*, *drosophila melanogaster*; *aq*, *amphimedon queenslandica*; *mb*, *monosiga brevicollis*; *dr*, *daneo rerio*; *xt*, *xenopus tropicalis*; *ce*, *caenorhabtidis elegans*; *ma*, *methanosaccrina acetovirans*; *at*, *arabidopsis thaliana.* Amino acid sequences are: *rn*NKCC1 (GenBank ID: NP_113986.1), *rn*NKCC2 (GenBank ID: NP_062007.2), *rn*NCC (GenBank ID: NP_062218.3), *rn*KCC1 (GenBank ID: NP_062102.1), *rn*KCC2 (GenBank ID: NP_599190.1), *rn*KCC3 (GenBank ID: NP_001103100.1), *rn*KCC4 (GenBank ID: NP_001013162.2), *rn*CIP1 (GenBank ID: Q66HR0.1), *rn*CCC9 (GenBank ID: EDM11357.1), *xt*KCC (GenBank ID: NP_001072306.2), *dr*KCC (GenBank ID: XP_701000.4), *dm*KCC (GenBank ID: NP_726378.1), *ce*KCC (GenBank ID: ACN62948.1), *aq*KCC (GenBank ID: XP_003384645.1), *mb*KCC (GenBank ID: XP_001743661.1), *at*KCC (GenBank ID: AAF19744.1), and *ma*CCC (GenBank ID: NP_619366.1).

2. Materials and methods

2.1. Site-directed mutagenesis

Site directed mutagenesis was performed according to the Quick-Change mutagenesis system (Stratagene, Heidelberg, Germany), using a previously reported rat KCC2b (GenBank ID: NM_134363) expression clone [18]. Oligonucleotides for the generation of the mutations were as follows (only forward primers are given): $KCC2_{Q673A}$ 5′-CCAGCACCAGTAGCGCGGGCCTCCAGTTCT-3′, $KCC2_{L674A}$ 5′CTGGAGGCCCCAGGCACTGGTGCTGGTG-3′, $KCC2_{L675A}$ 5′TGGAGGCCCCAGCTAGCGGTGCTGGTGC-3′; $KCC2_{V676A}$ 5′-CCCCAG CTACTGGCGCTGGTGCGTGTG-3′. All generated clones used in this study were confirmed by sequencing.

2.2. Determination of K^+–Cl^- cotransport

Transport activity was determined by measuring Cl^--dependent uptake of $^{86}Rb^+$ (PerkinElmer Life Sciences Life Sciences) in HEK-293 cells [22]. Cells were cultured in DMEM (Invitrogen) and transfected using TurboFect (Fermentas, St. Leon-Roth, Germany). Cells were harvested 40 h after transfection and transferred into poly-L-lysine-coated wells of a six well culture dish and incubated for 3 h. After removal of the medium, cells were incubated in 1 ml preincubation buffer (100 mM N-methyl-D-glucamine-chloride, 5 mM KCl, 2 mM $CaCl_2$, 0.8 mM $MgSO_4$, 5 mM glucose, 5 mM HEPES, pH 7.4, 0.1 mM ouabain) for 15 min at room temperature. A 10 min uptake period in preincubation buffer supplemented with 1 μCi/ml $^{86}Rb^+$ at room temperature followed. At the end of the uptake period, cells were washed three times in 1 ml ice-cold preincubation buffer without ouabain to remove extracellular tracer. Cells were lysed in 500 μl 0.25 M NaOH for 1 h and then neutralized with 250 μl pure acetic acid. $^{86}Rb^+$ uptake was assayed by Cerenkov radiation, and the protein amount was determined by BCA (Thermo Fisher Scientific, Bonn, Germany).

In some experiments, non-radioactive flux measurements based on thallium (Tl^+)-mediated Fluozin-2 fluorescence were performed [18,23]. 24 h after transfection, HEK-293 cells were plated in poly-L-lysine-coated wells of a 96-well culture dish, black-walled with clear bottom (Greiner Bio-One) at a concentration of 100,000 cells/well. The next day, the medium was replaced by 80 μl of preincubation buffer (100 mM *N*-methyl-D-glucamine chloride, 5 mM KCl, 2 mM $CaCl_2$, 0.8 mM $MgSO_4$, 5 mM glucose, 5 mM HEPES, pH 7.4) containing 2 μM Flouzin-2 dye (Invitrogen) plus 0.2% (w/v) Pluronic F-127 (Invitrogen). Cells were incubated at room temperature for 48 min. Afterwards, the cells were washed three times with 80 μl of preincubation buffer and incubated for 15 min with 80 μl of preincubation buffer plus 0.1 mM ouabain. The cell plate was inserted into a fluorometer (Fluoroskan Accent, Thermo Scientific, Bremen, Germany), and the wells were injected with 40 μl of thallium stimulation buffer (12 mM Tl_2SO_4, 100 mM NMDG, 5 mM Hepes, 2 mM $CaSO_4$, 0.8 mM $MgSO_4$, 5 mM glucose, pH 7.4). The fluorescence was measured in a kinetic-dependent manner (excitation, 485 nm; emission, 538 nm; 1 frame in 5 s in a 200-s time span). The activity was calculated with the initial values of the slope of Tl^+-stimulated fluorescence increase by using linear regression.

In addition, expression of the respective construct was determined for each flux measurement by immunoblot analysis or immunocytochemistry. At least three biological and three technical replicas were performed for each experiment. Data are given as mean ± standard deviation. Significant differences between the groups were analyzed by a Student's *t*-test.

2.3. Immunocytochemistry

For immunocytochemistry, transfected cells were seeded on 0.1 mg/ml poly-L-lysine-coated coverslips. After 36 h, cells were fixed with 4% paraformaldehyde in 0.2 M phosphate buffer for 10 min. After fixation, cells were washed three times with phosphate-buffered saline (PBS) and incubated with blocking solution (0.3% Triton X-100, 3% bovine serum albumin, 11% goat serum in PBS) for 30 min at room temperature. Cells were then incubated with primary antibody N1/12 (NeuroMab, Davis, USA), diluted 1:500 in carrier solution (0.3% Triton X-100, 1% bovine serum albumin, 1% goat serum in PBS) for 1 h and washed three times with PBS for 5 min. After transfer in carrier solution, cells were treated

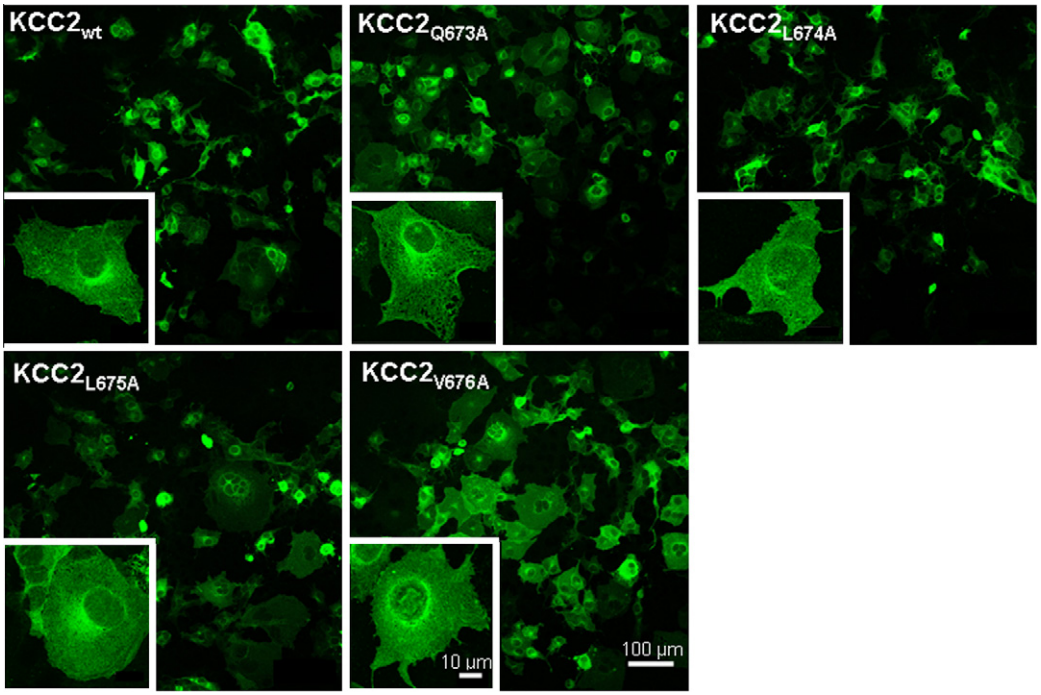

Fig. 2. Immuncytochemical labeling of KCC2 in COS-7 cells. COS-7 cells were transiently transfected with $KCC2_{wt}$ or KCC2 mutants ($KCC2_{Q673A}$, $KCC2_{L674A}$, $KCC2_{L675A}$ and $KCC2_{V676A}$). KCC2-ir revealed that all mutants were located at the plasma membrane and the perinuclear regions in a pattern indistinguishable from $KCC2_{wt}$. Photomicrographs were taken by confocal laser scanning microscopy with a 63x or a 20x objective (Leica TCS SP2).

with the secondary antibody (goat anti-rabbit conjugated to Alexa Fluor 488, diluted 1:1000, Invitrogen, Darmstadt, Germany). After washing, cells were mounted onto glass slides with Vectarshield Hard Set (Vector Laboratories, Burlingame, CA). Photomicrographs were taken by confocal laser scanning microscopy with a 63× and 20× objectives (Leica TCS SP2).

2.4. Cell-surface protein labeling

To detect cell surface expression of $KCC2_{wt}$ and $KCC2_{L675A}$, transfected cells were seeded on 0.1 mg/ml poly-L-lysine-coated coverslips. After 40 h, cells were incubated on ice and washed twice with ice-cold PBS. After incubation with 10 µg/ml Alexa 633-labeled wheat-germ agglutinin (WGA, Invitrogen) for 30 min on ice, cells were washed with ice-cold PBS. After fixation with 4% paraformaldehyde in 0.2 M phosphate buffer for 10 min, cells were incubated with primary and secondary antibody as described before. Colocalization between WGA-ir and KCC2-ir were analyzed with the software ImageJ and the plug-in OBCOL. At least 20 cells were analyzed for each construct. Data are given as mean ± standard deviation. Significant differences between the groups were analyzed by a Student's *t*-test.

3. Results

3.1. Evolutionary conservation of the $_{673}QLLV_{676}$ residues in the β1 strand of the C-terminus

The six amino acids of the β1 strand of KCC2 displayed the highest conservation in multiple sequence alignments of the C-terminus from mammalian CCCs, distantly related KCCs and *ma*CCC (Suppl. Fig. 1). The only exception was CCC9 where none of the amino acids was conserved (Fig. 1). The protein identity of the β1 strand was 4-fold increased (66.7%) between *rn*KCC2 and *ma*CCC compared to the entire C-terminus (16.5%). Within the β1 strand,

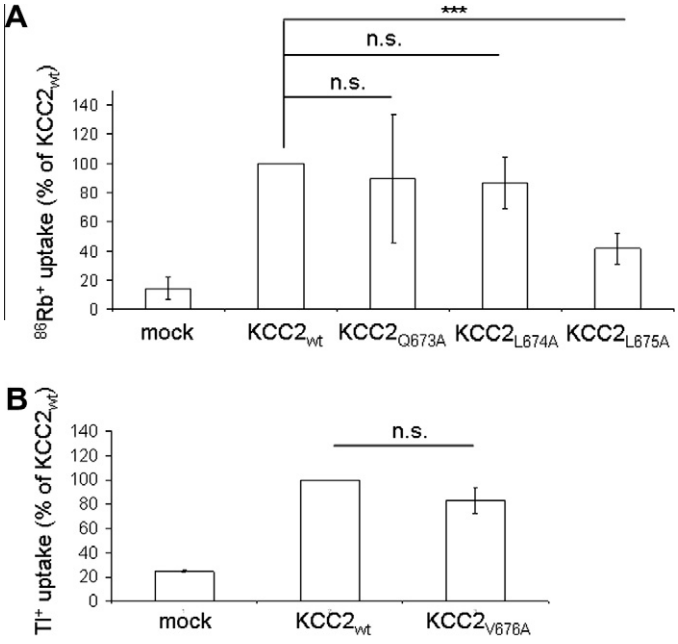

Fig. 3. Mutations in $_{673}QLLV_{676}$ differentially affect transport activity of KCC2. HEK-293 cells were transiently transfected 40 h prior flux measurements. An empty vector was used for mock transfection. Flux measurements were performed by $^{86}Rb^+$ uptake (A) and Tl^+ uptake (B). $KCC2_{Q673A}$, $KCC2_{L674A}$ and $KCC2_{V676A}$ exhibited normal transport activity. In contrast $KCC2_{L675A}$ displayed a 2.4-fold significant decrease of the transport activity (41.4 ± 10.6%, $p = 7.9 \times 10^{-7}$) compared to $KCC2_{wt}$. Values represent mean ± s.d. of at least 3 independent measurements. ns, none significant ($p > 0.05$); $^{***}p < 0.001$.

the first four residues (*rn*KCC2: $_{673}QLLV_{676}$) are the most highly conserved amino acids and three of them exist also in *ma*CCC. Evolutionary conservation was highest for $KCC2_{L675}$ (88.2%) followed by Q_{673} (82.4%), V_{676} (76.5%), and L_{674} (53%). The high conservation

of these residues across orthologs and paralogs in the structural β1 strand region of the C-terminus indicated a severe constraint on the sequence at this position.

3.2. Mutations of individual $_{673}$QLLV$_{676}$ residues differentially affect transport activity

To analyze the role of $_{673}$QLLV$_{676}$ residues for the transport activity of *rn*KCC2, we mutated them individually to alanine. This resulted in the four mutants KCC2$_{Q673A}$, KCC2$_{L674A}$, KCC2$_{L675A}$ and KCC2$_{V676A}$. To examine the functional consequences of the mutations, the constructs were transiently expressed in COS-7 cells and the expression was analyzed by immuncytochemistry. KCC2 immunoreactivity (KCC2-ir) of all mutants was detected at the plasma membrane and the perinuclear region (Fig. 2). The labeling pattern of the mutants was indistinguishable from KCC2 wild-type (KCC2$_{wt}$). These data indicate that single $_{673}$QLLV$_{676}$ mutations of KCC2 did not affect protein expression and localization.

Next, we determined the transport activity of KCC2 by $^{86}Rb^+$ or Tl^+ flux measurements in HEK-293 cells. To eliminate any uptake through endogenous NKCC1, the experiments were performed in Na^+-free solution with *N*-methyl-D-glucamine being the replacement cation (Gagnon 2006, Hartmann 2010). HEK-293 cells transiently transfected with KCC2$_{wt}$ exhibited a significant higher $^{86}Rb^+$ and Tl^+ uptake (100%) compared to mock-transfected control cells (14.3 ± 7.8% and 24.7 ± 0.85%) (Fig. 3). The mutant KCC2$_{L675A}$ displayed a 2.4-fold significant decrease of the transport activity (41.4 ± 10.6% residual activity, $p = 7.9 \times 10^{-7}$) compared to KCC2$_{wt}$ (Fig. 3A). The transport activities of KCC2$_{Q673A}$ (89.6 ± 44.23%, $p = 0.7$), KCC2$_{L674A}$ (86.4 ± 17.7%, $p = 0.17$) and KCC2$_{V676A}$ (83.4 ± 10.7%, $p = 0.13$) were not significantly different from KCC2$_{wt}$ (Fig. 3). Taken together, these results identify L$_{675}$ as a critical residue for KCC2 transport activity.

3.3. Cell surface expression of KCC2$_{L675A}$ is not altered

Of the four mutations, only KCC2$_{L675A}$ impaired transport activity. Our immunocytochemical analyses in COS-7 cells had indicated normal subcellular distribution (Fig. 2). To rule out that KCC2$_{L675A}$ behaved differentially between HEK-293 cells (flux measurements) and COS-7 cells (expression analysis), we performed immunocytochemical analysis in HEK-293 cells as well. Again, no difference was observed between KCC2$_{wt}$ and KCC2$_{L675A}$ (data not shown). To investigate surface expression of the mutant in more detail, WGA-surface labeling was performed (Solé et al. 2009) (Fig. 4). Quantitative pixel-by-pixel analysis revealed similar colocalization of KCC2$_{wt}$ (100 ± 23.4%) or KCC2$_{L675A}$ (98.6 ± 23.1%) with WGA in the plasma membrane. These data suggest that mutation of L$_{675}$ alters the conformation of KCC2 without affecting surface expression.

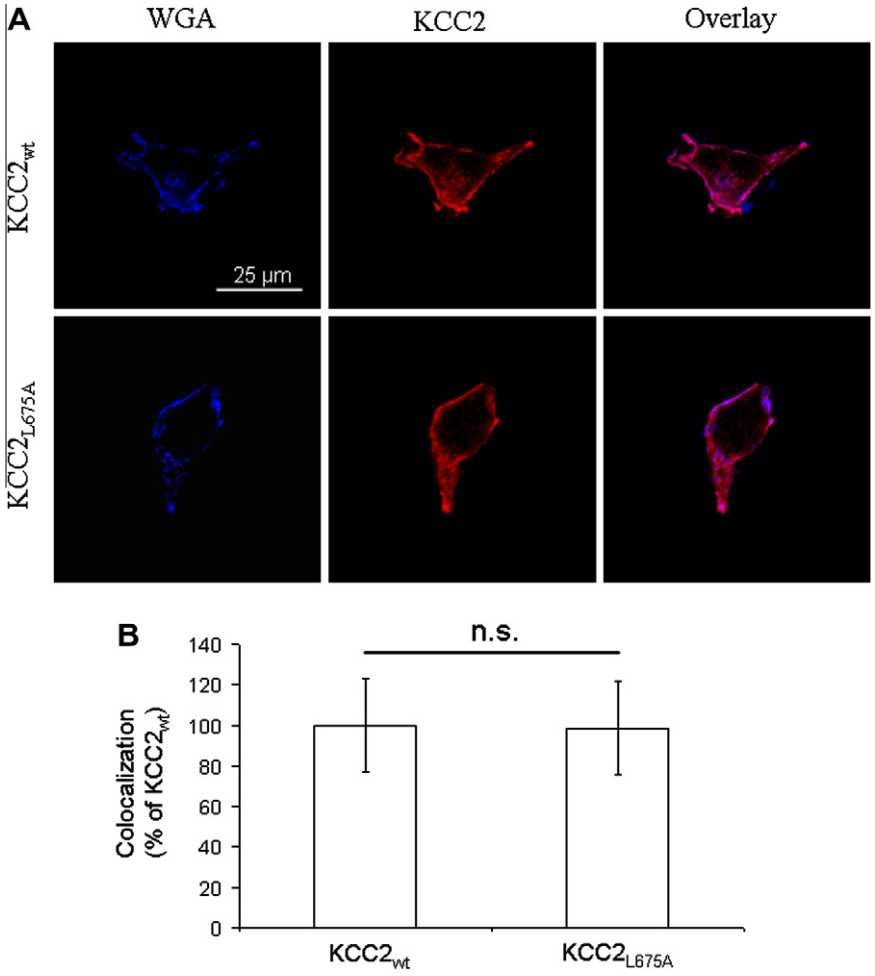

Fig. 4. Cell surface expression of KCC2$_{L675A}$ is not altered. HEK-293 cells were transiently transfected with KCC2$_{wt}$ and KCC2$_{L675A}$. Cell surface expression of KCC2 was analyzed through colocalization studies with WGA. Confocal images demonstrated a similar colocalization of KCC2$_{wt}$ and KCC2$_{L675A}$ with WGA (A). The relative cell surface expression of KCC2$_{wt}$ or KCC2$_{L675A}$ was analyzed by pixel-by-pixel intensities of confocal images using ImageJ software (B). Values represent mean ± s.d. of at least 20 cells. ns, none significant ($p > 0.05$).

4. Discussion

Here, we identified L_{675} within the C-terminal β1 strand as a critical amino acid residue for KCC2 transport activity. The β1 sequence is located between the TMDs and a presumed dimerization interface, consisting of the α helices 1 and 2 [13]. Both areas have been implicated in oligomerization of KCCs [11,13,24,25]. Thus, the high evolutionary sequence conservation of the β1 sequence was suggested to reflect the requirement of proper orientation of the α helices 1 and 2 with respect to the nearby TMDs. Mutation of L_{675} might therefore compromise dimerization, which is required for transport-activity [8,11]. Due to the formation of KCC2 aggregates in heterologous expression systems during biochemical purification [26,27], we were not able to investigate the oligomeric status of $KCC2_{L675A}$.

Other effects of the mutation might also be considered. The β1 sequence is at the surface of the molecule [13] and a binding site of the AP-2 complex is located in close proximity ($_{657}$LLXXEE$_{662}$) [28]. The β1 strand might therefore be involved in regulating endocytosis. We did, however, not observe any difference in the subcellular localization of $KCC2_{L675A}$ using immunocytochemistry and WGA surface labeling. These results argue against altered internalization. It is therefore most likely that mutation of L_{675} has an impact on the conformation of KCC2. This observation is in line with other point mutations that only impair transport activity without affecting surface expression of KCC2 [18,19].

Three out of four mutants displayed no change in transport activity, protein expression or localization. This was despite the fact that the mutations addressed extremely conserved amino acids. Several explanations might account for this observation. We substituted aliphatic (valine, leucine) or polar (glutamine) amino acid residues by the tiny amino acid alanine. This amino acid was chosen because of its absence in the analyzed positions in the *bona-fide* N(K)CC and KCC transporters. We cannot exclude that more severe amino acid replacements might have entailed functional consequences. Substitution of Y_{1087} by different amino acids, for instance, resulted in strikingly different phenotypes [19]. However, the phenotype of the L_{675} mutation to alanine indicates that our substitution strategy was well suited to identify sequence constraints. Previously, a different requirement of four evolutionary highly conserved cysteines in the LEL between the closely related KCC2 and KCC4 was reported [18]. Whereas loss of these cysteines abolished KCC2 transport activity, the same substitutions were well tolerated in KCC4. These data demonstrate a striking variability in sequence constraints even between closely related CCC members. It is therefore possible, that other CCC family members are more sensitive to mutations in these three amino acid residues in the β1 strand.

In summary, the identification of L_{675} as an important amino acid residue provides novel insights into the structural requirements of the C-terminus for KCC2 transport activity. In addition, our data indicate a surprisingly low sequence constraint in the β1 strand. Whether this is specific to KCC2, or holds true for other CCC family members as well will be an important topic for future studies to better understand the extreme evolutionary conservation of the β1 sequence. Finally, this study demonstrates the utility of structural information and evolutionary analysis to identify important amino acid residues in CCC members.

Acknowledgments

We thank Martina Reents for excellent technical support and Sina Lenski for help in generation of some constructs. This work was supported by grants from the Deutsche Forschungsgemeinschaft (No428/4-1 to H.G.N.).

Appendix A. Supplementary data

Supplementary data associated with this article can be found, in the online version, at doi:10.1016/j.bbrc.2012.02.147.

References

[1] G. Gamba, Molecular physiology and pathophysiology of electro neutral cation-chloride cotransporter, Physiology Review 85 (2005) 423–493.
[2] N.D. Daigle, G.A. Carpentier, R. Frenette-Cotton, M.G. Simard, M.-H. Lefoll, M. Noel, L. Caron, J. Noel, P. Isenring, Molecular characterization of a human cation-Cl^- cotransporter (SLC12A8A, CCC9A) that promotes polyamine and amino acid transport, Journal of Cellular Physiology 220 (2009) 680–689.
[3] C. Rivera, J. Voipo, J.A. Payne, E. Ruusuvuori, H. Lahtinen, K. Lamsa, U. Pirvola, M. Saarma, And Kaila, K, The K^+/Cl^- co-transporter KCC2 renders GABA hyperpolarizing during neuronal maturation, Nature 397 (1999) 251–255.
[4] W. Jarolimek, A. Lewen, U. Misgeld, A furosemide-sensitive K^+–Cl^- cotransporter counteracts intracellular Cl^- accumulation and depletion in cultured rat midbrain neurons, The Journal of Neuroscience 19 (1999) 4695–4704.
[5] C.A. Hübner, V. Stein, I. Hermans-Borgmeyer, T. Meyer, K. Ballanyi, T.J. Jentsch, Disruption of KCC2 reveals an essential role of K–Cl cotransport already in early synaptic inhibition, Neuron 30 (2001) 515–524.
[6] V. Balakrishnan, M. Becker, S. Löhrke, H.G. Nothwang, E. Güresir, E. Friauf, Expression and function of chloride transporters during development of inhibitory neurotransmission in the auditory brainstem, The Journal of Neuroscience 23 (2003) 4134–4145.
[7] A. Reynolds, E. Brustein, M. Liao, A. Mercado, E. Babilonia, D.B. Mount, P. Drapeau, Neurogenic role of the depolarizing chloride gradient revealed by global overexpression of KCC2 from the onset of development, The Journal of Neuroscience 28 (2008) 1588–1597.
[8] P. Blaesse, I. Guillemin, J. Schindler, M. Schweizer, E. Delpire, L. Khiroug, E. Friauf, H.G. Nothwang, Oligomerization of KCC2 correlates with development of inhibitory neurotransmission, The Journal of Neuroscience 26 (2006) 10407–10419.
[9] N.-S. Woo, J. Lu, R. England, R. McClellan, S. Dufour, D.B. Mount, A.Y. Deutch, D. Lovinger, E. Delpire, Hyperexcitability and epilepsy associated with disruption of the mouse neuronal-specific K–Cl cotransporter gene, Hippocampus 12 (2002) 258–268.
[10] J. Tornberg, V. Voikar, H. Savilahti, H. Rauvala, M.S. Airaksinen, Behavioural phenotypes of hypomorphic KCC2-deficient mice, European Journal of Neuroscience 21 (2005) 1327–1337.
[11] S. Casula, B.E. Shmukler, S. Wihelm, A.K. Stuart-Tilley, W. Su, M.N. Chernova, C. Brugnara, S.L. Alper, A dominant negative mutant of the KCC1 K–Cl cotransporter, The Journal of Biological Chemistry 276 (2001) 41870–41878.
[12] J.C. De Jong, P.H.G.M. Willems, F.J.M. Mooren, L.P.W.J. Van den Heuve, N.V.A.M. Knoers, R.J.M. Bindels, The structural unit of the Thiazide-sensitive NaCl cotransporter is a homodimer, The Journal of Biological Chemistry 278 (2003) 24302–24307.
[13] S. Warmuth, I. Zimmermann, R. Dutzler, X-ray structure of the C-terminal domain of a prokaryotic cation-chloride cotransporter, Structure 17 (2009) 538–546.
[14] P. Isenring, B. Forbush, Mutagenic mapping of the Na–K–Cl cotransporter for domains involved in ion transport and bumetanide binding, Journal of General Physiology. 112 (1998) 549–558.
[15] P. Isenring, S.C. Jacoby, B. Forbush, The role of transmembrane domain 2 in cation transport by the Na–K–Cl cotransporter, Proceedings of the National Academy of Sciences USA 95 (1998) 7179–7184.
[16] P. Isenring, B. Forbush, Ion transport and ligand binding by the Na–K–Cl cotranporter, structure-function studies, Comparative Biochemistry and Physiology Part A 130 (2001) 487–497.
[17] M.J. Bergeron, K.B.E. Gagnon, L. Caron, P. Isenring, Identification of Key functional domains in the C terminus of the K^+–Cl^- cotransporters, The Journal of Biological Chemistry 281 (2006) 15959–15969.
[18] A.-M. Hartmann, M. Wenz, A. Mercado, C. Störger, D.B. Mount, E. Friauf, H.G. Nothwang, Differences in the large extracellular loop between the K^+–Cl^- cotransporters KCC2 and KCC4, The Journal of Biological Chemistry 285 (2010) 23994–24002.
[19] K. Strange, T.D. Singer, R. Morrison, E. Delpire, Dependence of KCC2 K–Cl cotransporter activity on a conserved carboxy terminus tyrosine residue, American Journal of Physiology Cell Physiology 279 (2000) 860–867.
[20] J. Rinehart, Y.D. Maksimova, J.E. Tanis, K.L. Stone, C.A. Hodson, J. Zhang, M. Risinger, W. Pan, D. Wu, C.M. Colangelo, B. Forbush, C.H. Joiner, E.E. Gulcicek, P.G. Gallagher, R.P. Lifton, Sites of regulated phosphorylation that control K–Cl cotransporter activity, Cell 138 (2009) 525–536.
[21] A. Mercado, V. Broumand, K. Zandi-Nejad, A.H. Enck, D.B. Mount, A C-terminal domain in KCC2 confers constitutive K^+–Cl^- cotransporter, The Journal of Biological Chemistry 281 (2006) 1016–1026.
[22] A.-M. Hartmann, H.G. Nothwang, Opposite temperature effect on transport activity of KCC2/KCC4 and N(K)CCs in HEK-293 cells, BMC Research Notes 4 (2011) 526.
[23] E. Delpire, E. Days, L.M. Lewis, D. Mi, K. Kim, C.W. Lindsley, C.D. Weaver, Small-molecule screen identifies inhibitors of the neuronal K–Cl cotransporter KCC2, Proceedings of the National Academy of Sciences USA 106 (2009) 5383–5388.

[24] C.F. Simard, M.J. Bergeron, R. Frenette-Cotton, G.A. Carpentier, M.-E. Pelchat, L. Caron, P. Isenring, Homooligomeric and heterooligomeric associations between K+–Cl^- cotransporte isoforms and between K^+–Cl^- and Na^+–K^+–Cl^- cotransporter, The Journal of Biological Chemistry 282 (2007) 18083–18093.
[25] S. Casula, A.S. Zolotarev, A.K. Stuart-Tilley, S. Wilhelm, B.E. Shmukler, C. Brugnara, A.L. Alper, Chemical cross linking studies with the mouse KCC1 K–Cl cotransporter, Blood Cells, Molecules, and Diseases 42 (2009) 233–240.
[26] P. Uvarov, A. Ludwig, M. Markkanen, S. Soni, C.A. Hübner, C. Rivera, M.S. Airaksinen, Coexpression and heteromerization of two neuronal K–Cl cotransporter isoforms in neonatal brain, Journal of Biological Chemistry 284 (2009) 13696–13704.
[27] A.-M. Hartmann, P. Blaesse, T. Kranz, M. Wenz, A.F. Schinder, K. Kaila, E. Friauf, H.G. Nothwang, Opposite effect of membrane raft perturbation on transport activity of KCC2 and NKCC1, Journal of Neurochemistry 111 (2009) 321–331.
[28] B. Zhao, A.Y.C. Wong, A.M. Murshid, D. Bowie, J.F. Presley, F.K. Bedford, Identification of a novel di-leucine motif mediating K^+/Cl^- cotransporter KCC2 constitutive endocytosis, Cellular Signalling 20 (2008) 1769–1779.
[29] J.D. Thompson, D.G. Higgins, T.J. Gibson, Clustal W: improving the sensitivity of progressive multiple sequence alignment through sequence weighting, position-specific gap penalties and weight matrix choice, Nucleic Acid Research 22 (1994) 4673–4680.